

# Apparent Hydrodynamic Thickness of Densely Grafted Polymer Layers in a Theta Solvent

YOON-KYOUNG CHO, ALI DHINOJWALA, STEVE GRANICK

University of Illinois, Department of Material Science and Engineering, 105 S. Goodwin Ave., Urbana, Illinois 61801

Received 16 July 1997; revised 13 August 1997; accepted 13 August 1997

**ABSTRACT:** We study the drainage of a near-theta solvent through densely grafted polymer layers and compare to recent notions that these layers display little permeability to solvent flow at surface separations less than a “hydrodynamic thickness.” The solvent is trans-decalin (a near-theta solvent at the experimental temperature of 24°C). The polymer is polystyrene (PS) end-attached to two opposed mica surfaces via the selective adsorption of the polyvinylpyridine (PVP) block of a PS-PVP diblock copolymer. The experimental probe was a surface forces apparatus modified to apply small-amplitude oscillatory displacements in the normal direction. Out-of-phase responses reflected viscous flow of solvent alone—the PS chains did not appear to contribute to dissipation over the oscillation frequencies studied. The value of the hydrodynamic thickness ( $R_H$ ) was less than the coil thickness ( $L_o$ ) measured independently from the onset of surface–surface interactions in the force–distance profile, implying significant penetration of the velocity field into the polymer layer. As the surface–surface separation was reduced from  $3L_o$  to  $0.3L_o$ , the apparent hydrodynamic thickness ( $R_H^*$ ) decreased monotonically to values  $R_H^* \ll R_H$ . Physically, this indicates that the “slip plane” moved progressively closer to the solid surfaces with decreasing surface–surface separation. This was accompanied by augmentation of the effective viscosity by a factor of up to approximately 5, indicating somewhat diminished permeability of solvent through the overlapping polymer layers. Similar results hold for the flow through surface-anchored polymers in a good solvent. It is interesting to note the strong stretching of densely end-grafted polymers in a theta solvent. © 1997 John Wiley & Sons, Inc. *J Polym Sci B: Polym Phys* **35**: 2961–2968, 1997

**Keywords:** anchored coils; hydrodynamic thickness; surface forces apparatus; interfacial rheology; interface; viscosity; theta solvent

## INTRODUCTION

Just as polymer coils in solution diffuse constantly towards or away from one another, giving rise to hydrodynamic interactions that have been much discussed,<sup>1,2</sup> so also do polymer-laden colloidal surfaces often enter into relative motion towards or away from one another. Therefore, the process of steric stabilization includes serious hydrodynamic influences.

Past work on surface–surface interactions mediated by steric forces of surface-attached polymers has focused on equilibrium force–distance profiles and on the dynamic viscoelastic shear forces.<sup>3–5</sup> The dependence of these static forces on molecular weight, surface coverage, and interaction energies is well documented and extensively studied.<sup>6–9</sup> Much less is understood about polymer-coated surfaces for relative motion in the direction normal to the surfaces.

We are interested here in hydrodynamic forces due to drainage of solvent between polymer-coated surfaces in a theta solvent. Simple considerations show that for typical Brownian motion

Correspondence to: S. Granick

*Journal of Polymer Science: Part B: Polymer Physics*, Vol. 35, 2961–2968 (1997)  
© 1997 John Wiley & Sons, Inc. CCC 0887-6266/97/172961-08

of colloidal particles, the magnitude of hydrodynamic forces can often exceed the static forces. How, then, are hydrodynamic forces of polymer-laden surfaces in close proximity modified by the presence of polymer from predictions from the classical views that are based on continuum hydrodynamics?

The traditional approach to account for the presence of adsorbed or grafted polymers is simply to take the classical Reynolds equation for describing hydrodynamic forces<sup>10</sup> and to subtract, from the actual solid–solid distance, the effective thickness of the immobilized polymer layer. This is often referred to as hydrodynamic thickness.<sup>9,11,12</sup> This patchwork approach works if the solid–solid separation is much greater than the hydrodynamic thickness. However, at lesser separations, even if polymer-coated surfaces do not touch one another, hydrodynamic forces are found experimentally to be smaller than expected from such a modified Reynolds equation.<sup>9,11,12</sup> Surely, the reason is that a surface-attached polymer layer is far from a rigid substrate; the hydrodynamic forces can be large enough to influence the penetration of the solvent velocity field within the adsorbed layer, as we shall see from the study below. In other language, the “slip plane”<sup>11</sup> shifts with changes of the surface–surface separation. As we explain below, several earlier studies of the hydrodynamic thickness of adsorbed polymers<sup>9,11</sup> suffer from the limitation that elastic and dissipative forces were not distinguished from one another, although Klein<sup>13</sup> mentions this difficulty, concluding that corrections would be insignificant. We find that failure to distinguish elastic from dissipative forces renders problematical the significance of earlier comparisons to theoretical predictions for dissipative forces. The present study, which concerns drainage of a theta solvent, builds on our recent study that concerned drainage of a good solvent.<sup>14</sup>

## EXPERIMENTAL

The diblock copolymers of polystyrene and poly-2-vinylpyridine (PS-PVP) were purchased from Polymer Source Inc. (Quebec, Canada). The molecular weights of the blocks were 55,400 g/mol (PS) and 9,200 g/mol (PVP). The ratio of weight-average to number-average molecular weight was  $M_w/M_n = 1.03$ .

The block copolymers were allowed to adsorb from the good solvent, toluene, because the poly-

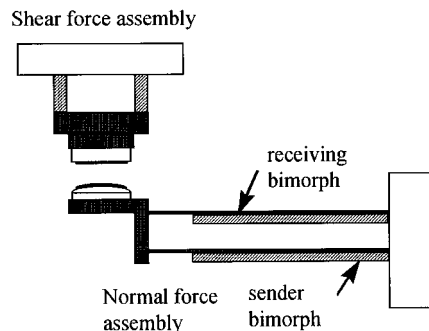


**Figure 1.** A schematic diagram of the apparatus to measure shear and normal forces concurrently. The top surface was attached to a shear force assembly described elsewhere (see text). The bottom surface was similarly attached to two piezoelectric bimorphs that were oriented at right angles to the normal line between the two surfaces. Oscillatory normal forces were generated by applying voltage to the bottom piezoelectric bimorph (the “sender”). This was resisted by the sample and the actual time-dependent deflection of the bottom surface was monitored from the time-dependent voltage that was induced in the top bimorph (the “receiver”).

mer could not be dissolved to a sufficiently high concentration in trans-decalin. Solutions were prepared in toluene at concentrations 5–10  $\mu\text{g}/\text{mL}$  (far below the critical micelle concentration). To ensure complete dissolution, the solutions were made at least 24 h before the subsequent adsorption process. Freshly cleaved sheets of muscovite mica were first calibrated in a surface forces apparatus to determine the mica thickness, then immersed in the polymer solution for 2 h. Because toluene is a nonsolvent for the PVP block but a good solvent for the PS block, the block polymers adsorbed onto the mica by selective adsorption of the PVP block. After adsorption, to rinse off nonadsorbed chains, the coated mica sheets were soaked in pure toluene for at least 2 h, then the chains were dried under flowing argon gas. Finally a droplet of trans-decalin was added to the polymer-coated sheets after they were mounted into the experimental apparatus. The experimental temperature was 24°C, 4° above the theta temperature for the bulk solution.

A schematic diagram of the interfacial rheometer, modified by means of a double cantilever bimorph assembly to apply small-amplitude oscillatory pumping in the normal direction, is shown in Figure 1. The top surface was held fixed in space and the bottom surface, fixed to a double cantilever spring comprised of two piezoelectric bi-

morphs, was pumped in the normal direction with small-amplitude oscillatory force (corresponding to displacements of 5–10 Å). The methods to analyze the dynamic mechanical data were analogous to those used for shear experiments; these methods have been described in detail elsewhere.<sup>4,15</sup> The main point is that a sinusoidally oscillating force is applied to a “sender” piezoelectric bimorph, and the damping and phase shift of oscillation are detected by a symmetrically placed “receiver” piezoelectric bimorph. The damping and phase shift of the oscillation can be related to the elastic and viscous force constant as follows.<sup>4,15</sup>

$$\omega b = K_{sp} A_o \sin(\theta) / A \quad (1)$$

$$k = K_{sp} (A_o \cos(\theta) / A - 1) \quad (2)$$

Here,  $A$  is the displacement in presence of liquid,  $A_o$  is the maximum displacement when surfaces are separated in air,  $\theta$  is the phase difference between the output when the surfaces are separated in air to that in presence of liquid, and  $K_{sp}$  is the effective spring constant of the normal force assembly. Equations (1) and (2) hold for measurements below the resonance frequency of the normal force assembly.

For the pumping experiments presented here,  $K_{sp} = 1 \times 10^4$  N/m (determined from the resonance frequency of the spring assembly and its known mass). The resonance frequency was 235 Hz. Linear response, obtained with oscillation amplitudes of < 1 nm, was verified. A weaker spring, with stiffness 900 N/m, was used to measure the static force–distance profile.

## RESULTS AND DISCUSSION

### Characterization of the Polymer Layers

To make contact with numerous past discussion of static force–distance profiles,<sup>8,9</sup> the force–distance profile was measured first. We are indebted to Lenore Cai for this measurement. In Figure 2, force normalized by the mean radius of curvature of the crossed cylinders is plotted against mica–mica separation on semi-logarithmic scales. The force was monotonically repulsive. As illustrated in Figure 2, the force–distance relation could be fit nearly quantitatively to the Alexander–de Gennes prediction with scaling exponents adjusted to correspond to the case of polymer brushes in a theta solvent.<sup>8,9</sup> The onset of measur-

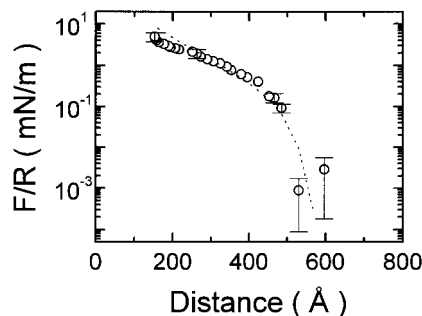


**Figure 2.** The static force that resisted compression ( $F$ ), normalized by the mean radius of curvature ( $R$ ) of the crossed cylindrical surfaces, plotted logarithmically against surface separation for the PS–PVP polymer in decalin. Dotted line shows fit to the Alexander–de Gennes prediction for brushes in a theta solvent. Error bars (relatively large for small repulsive forces, relatively low for large repulsive forces) are shown.

able surface forces occurred at 560 Å, which indicates that the thickness of the polymer layer was approximately four times the estimated end-to-end distance,  $R_o$  (71 Å) or 10 times the estimated radius of gyration,  $R_g$ , ( $L_o \sim 4R_o \sim 10R_g$ ) of polystyrene of this same molecular weight in a theta solvent.<sup>16</sup> The data here for the smallest forces show the point at which data points began to deviate from the baseline, and error bars are indicated. If we identify this thickness at the onset of repulsion as layer thickness, this implies a thickness  $L_o = 280$  Å per layer. It is interesting to note the strong stretching of densely end-grafted polymers in a theta solvent.

Because of the possibility that not only the PVP block but also the PS block would adsorb to mica, control experiments were also performed to measure the force–distance profile of adsorbed PS homopolymer of similar molecular weight.<sup>17</sup> Although PS did adsorb, the magnitude of the forces in the force–distance profile was considerably less at a given film thickness and the thickness of the adsorbed layer was less by the large factor of 3. We, thus, expect a brush-like structure for the adsorbed PS–PVP diblock copolymers, although the fact of having brush structure is actually incidental to the main point of the experiments that follow. Indeed, elsewhere we have contrasted the force–distance profile shown here with that measured when a single PS–PVP polymer layer was compressed against a bare mica surface.<sup>18</sup> The measured film thickness was roughly one-half in the latter case, as expected, because classical theories of brush force–distance profiles do not dis-

tinguish the cases of brush–brush and brush–mica contact.<sup>6–9</sup> This again indicates the brush structure of these layers.

The grafting density was determined from the thickness, measured in a surface forces apparatus, of two opposed PS-PVP layers after removing the decalin solvent by flowing dry argon through the apparatus for at least 3 h.<sup>17</sup> The grafting density was  $3.4 \times 10^{16}$  chains/m<sup>2</sup>, which corresponds to an average spacing of 54 Å between anchor points of the PS.

### Analysis of Data

For a Newtonian fluid, elastic forces in the frequency range studied should be negligible. However, for adsorbed polymer layers or a brush, the elastic force contribution is significant when the opposed layers touch each other. An additional contribution to the elastic forces also comes from the compliance of the device and from the glue used to mount the mica surfaces onto the device. To separate these contributions, the respective contributions of the hydrodynamic forces of the sample (an out-of-phase response), the static forces of the sample (an in-phase response), and the device itself (predominantly an in-phase response) were then separated by a model in which the response of the sample and of the device acted in parallel. Details of this model are discussed elsewhere in the context of making similar measurements of confined films in a shear geometry.<sup>4,15</sup>

### Dissipative (Out-of-Phase) Forces

Analysis was simplified by the fact that the polymer itself appeared to give negligibly small viscoelastic response over the frequencies studied, as manifested by frequency-independent elasticity. Other control experiments showed that the magnitude of the out-of-phase viscoelastic response was directly proportional to frequency, as expected for Newtonian response. For these reasons, we attribute the observed dissipation in these experiments to solvent flow.

The hydrodynamic force for a sphere approaching a flat surface at a constant velocity,  $v$ , can be expressed using the classical Reynolds equation as follows:

$$F_H = 6\pi R^2 \eta v / D \quad (3)$$

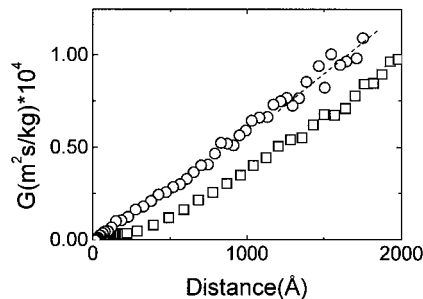


**Figure 3.** The viscous damping function,  $G$  (of order  $10^{-4}$  m<sup>2</sup>-s/kg) plotted against surface separation for pure trans-decalin (circles) and for trans-decalin between surfaces bearing adsorbed PVP–PB polymers (squares). The straight line corresponds to the known viscosity of trans-decalin. These values of  $G$  correspond to forces of order  $10^{-7}$  N. The oscillation frequency was 2.6 Hz. The inverse of the slope of  $G$  against surface separation implies the known viscosity of trans-decalin.

where  $R$  is the radius of the sphere,  $\eta$  is the viscosity, and  $D$  is the closest separation between the sphere and the flat surface.<sup>9,10,12–14,18,19,22</sup> For an oscillatory normal force, the hydrodynamic force constant can be written as:

$$\omega b_L = 6\pi R^2 \eta \omega / D \quad (4)$$

where  $b_L$  is an equivalent dashpot coefficient. For quantitative comparison to data<sup>9,12,14,20–22</sup> it is common to rewrite Eq. (4) as follows:

$$G = 6\pi R^2 \omega / (\omega b_L) = D / \eta \quad (5)$$

Thus, if  $G$  is plotted as a function of distance for a Newtonian fluid, the slope is the inverse viscosity and the  $D$  intercept is twice the hydrodynamic thickness. The latter, for small molecules, is typically within one molecular diameter.<sup>11,23,24</sup> It is essential to note that Eq. (5) involves only the dissipative force contribution,  $\omega b_L$ —not the total force as assumed in previous studies.

In Figure 3, having made this separation of dissipative forces from the total, we plot  $G$  as a function of surface–surface separation for two cases: bare mica surfaces immersed in pure decalin, and adsorbed PVP–PS polymer layers immersed in decalin. As should be expected, the inverse slope of the line is the same provided that  $D$  is large enough, indicating that the viscosity of the liquid was that of pure trans-decalin, 1.95 cP at 25°C. Deviations at smaller surface–surface separations are discussed below.

For the decalin solvent in the absence of poly-

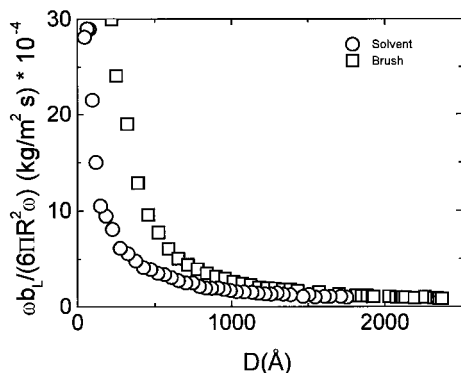


**Figure 4.** Same data as in Figure 3 but plotted as the hydrodynamic force constant,  $1/G$ , as a function of surface separation. Symbols are the same as in Figure 3.

mer, the Reynolds equation fits well. For the polymer layers, the hydrodynamic forces could also be fit to the Reynolds equation but with separation  $(D - 2R_H)$ , where  $R_H$  was an equivalent hydrodynamic thickness chosen to fit the data. At the largest separations studied the value of  $R_H$  was 200 Å, i.e., only two-thirds of the unperturbed thickness of the polymer layer ( $L_o \sim 280$  Å). It is interesting that this implied so much penetration of the solvent flow within the polymer coils.

The actual magnitude of the hydrodynamic forces is perhaps easier to understand intuitively. Therefore, for comparison, Figure 4 shows this quantity,  $1/G$ , plotted against surface–surface separation. One sees that hydrodynamic forces were indeed larger for polymer-coated surfaces; however, the quantitative analysis of fluid flow is more difficult in this form of representation.

### Lesser Separations

When the polymer layers were compressed to less than their unperturbed thickness the classical picture of a constant hydrodynamic thickness ceased to hold and the relation between  $G$  and  $D$  became strongly nonlinear. Others have also noted the nonlinear relation between  $G$  and  $D$  in this region.<sup>9,11,13</sup>

To analyze the decreased permeability of solvent in this regime, we sought to calculate an effective dynamic viscosity,  $\eta'$ , using Eq. (6),

$$\eta' = \omega b_L D / 6\pi R^2 \omega \quad (6)$$

This equation is obviously related to the classical Reynolds equation and its recent implementa-

tions.<sup>9,11,13,20,24</sup> The difficulty in implementing eq. (6) is to specify the relevant film thickness,  $D$ . First, we considered two unsatisfactory possibilities. If one took the actual surface–surface separation, this would be incorrect because the actual film thickness through which solvent flows is less than this; as discussed above, it is usual to estimate this as  $D - 2R_H$ , provided that the surface–surface separation is large enough. But, as the second possibility, if one assumed the same  $R_H$  as at large separation and calculated an effective  $\eta'$  from the slope of the line,  $G$  plotted against  $D$ , this would actually imply that the apparent viscosity decreased, the thinner the film. The results of both of these unreasonable calculations are plotted in Figure 5. Neither of these calculations would be physically meaningful.

This led us to consider the possibility that the effective hydrodynamic radius itself might change with film thickness. Perhaps, as the polymer layers began to overlap, the penetration of the flowing solvent into these layers changed from  $R_H$ , the limiting value at large surface–surface separation, to a lesser effective hydrodynamic radius,  $R_H^*$ , and larger effective viscosity,  $\eta'^*$ . The latter can be inferred either from the slope of  $G$  plotted against surface–separation (squares in Fig. 6), in which case the value of  $R_H^*$  is the intercept on the abscissa axis. Equivalently, one can calculate  $\eta'^*$

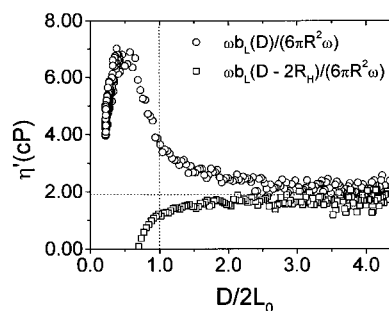


**Figure 5.** Inappropriate strategies to calculate the viscosity,  $\eta'$ , from the data in Figure 3. The failure of these approaches motivates the analyses presented in Figures 6 and 7. With the assumption that the effective shear rate should be calculated by normalizing the rate of motion by the total film thickness,  $\eta'$  would increase with decreasing film thickness (circles), but this calculation is incorrect because the actual film thickness through which solvent flows is known to be less than the total surface–surface separation. One could also seek to infer an effective  $\eta'$  using  $D - 2R_H$  instead of  $D$  in eq. (6) with the constant  $R_H$  evaluated at large surface–surface separations, but this would imply that  $\eta'$  decreased, the thinner the film (squares).

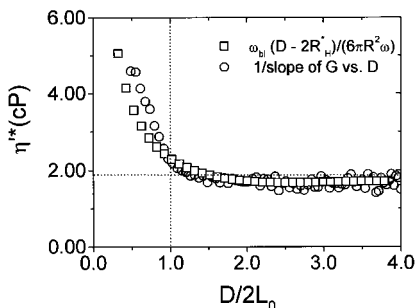


**Figure 6.** Apparent viscosity,  $\eta^*$ , plotted against the ratio of the actual surface–surface separation to the unperturbed thickness of the two polymer layers. Circles are from the slope of  $G$  plotted against surface–surface separation and squares are from eq. (6) using  $D - 2R_H^*$  with apparent hydrodynamic thickness,  $R_H^*$ , which is shown in Figure 7.

from eq. (6) using  $D - 2R_H^*$  instead of  $D$  (circles in Fig. 6). Figure 6 shows that the two approaches yield equivalent results.

In Figures 6 and 7, the implied  $\eta^*$  and  $R_H^*$  are plotted against the ratio of the actual surface–surface separation to the unperturbed thickness of the two polymer layers. Starting even before the layers touched one another,  $\eta^*$  (Fig. 6) began to rise monotonically. The rise in  $\eta^*$ , by a factor of up to 5, is reasonable when one considers that solvent diffusion slows somewhat with increasing polymer concentration.<sup>27</sup> The concomitant  $R_H^*$  (Fig. 7) decreased monotonically. One observes, in Figure 7, that  $R_H^*$  decreased from a constant value of 190 Å at large separations to less than 50 Å at the smallest separation. Another way to state this is that the solvent velocity field appeared to penetrate farther and farther within the layers, the more that they were compressed. It is interesting that  $R_H^*$  appears to extrapolate to zero at a finite surface–surface separation (190 Å); no interpretation is offered at this time.

Physically, the solvent flow in a compressed polymer matrix should involve elements of flow through a porous medium. Fredrickson et al.<sup>21</sup> analyzed the consequences for creeping flow of solvent through a porous medium of mesh size equal to the static correlation length in semidilute solution. Flow of solvent through a porous medium was modeled using the classical Brinkman Equation.<sup>25</sup> For the steady compression of strongly overlapped layers in semidilute concentration, the hydrodynamic force was then written as:

$$\omega b_L \propto (\eta \omega R^2)/D(D/\xi(D))^2 \quad (7)$$

where  $\xi$  is the hydrodynamic screening length and is not constant within the later. These arguments, formulated to describe chains in good solvent,<sup>21</sup> predict (if one substitutes  $\xi \propto (D)^{1.0}$  as expected in a theta solvent and a constant value of  $\eta$  throughout the crossed cylinder geometry) that  $G$  should scale as  $D^{1.0}$ .<sup>21</sup> But since the viscosity is not constant for compressed polymer layers and the average polymer concentration in our experiments reached the overlap concentration,  $c^*$ , only at a relatively large extent of compression,  $D/2L_0 \sim 0.3$ , it is probably not meaningful to compare to the present data. In this data, considerable modification of flow was observed at considerably lesser average concentration than semidilute.

It may at first seem surprising that the changes measured here were not larger; after all, the viscosity of PS solutions of similar concentrations would have increased to a level several orders of magnitude larger than the dilute solution viscosity. The important distinction is that the present experiment was predominantly sensitive to the viscous dissipation of the solvent during the pumping experiment and that the polymer molecules did not leave the gap during these measurements. The experiment was sensitive to permeability of solvent through the polymer layer<sup>26</sup> rather than long-range diffusion of polymer chains.

### Comparison With Good Solvent Conditions

Recently we performed similar experiments to measure the drainage of tetradecane (a good solvent) past polybutadiene (PB) polymers end-

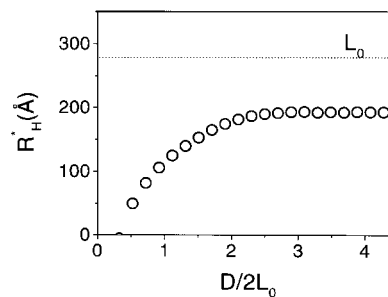


**Figure 7.** Apparent hydrodynamic thickness,  $R_H^*$ , calculated from Figure 3 by considering the  $x$ -intercept of the tangent of  $G$  vs.  $D$ , plotted against the ratio of the actual surface–surface separation to the unperturbed thickness of the two polymer layers. The data appear so smooth because they were calculated from a polynomial fit to the measured  $G$  shown in Figure 3.

attached to two opposed mica surfaces.<sup>14</sup> The PB was attached by selective adsorption of the polyvinylpyridine (PVP) block of a PB–PVP diblock copolymer. The molecular weights were 38,500 g/mol (PB) and 23,700 g/mol (PVP). The ratio weight-average to number-average molecular weight was  $M_w/M_n < 1.05$ . The dry layer thickness corresponded to  $2.3 \times 10^{16}$  chains/m<sup>2</sup>, an average spacing between anchor points of 65 Å. The onset of measurable surface forces occurred at  $2L_o = 1250$  Å, implying a thickness  $L_o = 625$  Å per unperturbed polymer layer. Because scatter in the data precluded determination of  $\eta'^*$  from the slope of  $G$  vs.  $D$ , the approximation was made that  $\eta'^*$  took the same value as for the bulk solvent.

Before comparing these experiments, some allowance must be made for differences in the molecular weight of the polymer chains and their grafting density. As a rough correction, the data were normalized as follows. First, the  $L_o$  for PB was normalized by the ratio of molecular weight in the two systems. In addition,  $R_H$  was normalized by the ratio of molecular weight times the ratio of grafting density ( $\Gamma$ ):

$$L'_{o,PB} = L_{o,PB} \times (M.W._{PS}/M.W._{PB}) \sim 1.4 L_{o,PB} \quad (8)$$

$$R'_{H,PB} = R_{H,PB} \times (M.W._{PS}/M.W._{PB}) \times (\Gamma_{PS}/\Gamma_{PB}) \sim 2.1 R_{H,PB} \quad (9)$$

Equation (8) expresses the fact that  $L_o$  is expected to be proportional to molecular weight.<sup>6</sup> Equation (8) was chosen to compare conditions in which the average segment concentration within the polymer layer would be constant.

The comparison of the present findings in near-theta solvent, with those findings in a good solvent after this normalization, is shown in Figure 8. The horizontal lines in Figure 8 support the expectation that the layer height should be substantially larger in the good solvent than the theta solvent. Moreover, when the surfaces were far apart, the hydrodynamic thickness was approximately the same as the unperturbed thickness of the polymer layer. Although the comparison according to solvent quality must be considered preliminary at this stage because of the limited amount of data, it is provocative to note that, in spite of rather thicker  $R_H^*$  in the good solvent condition, as the polymers were compressed, the dependence on film thickness of the two curves in

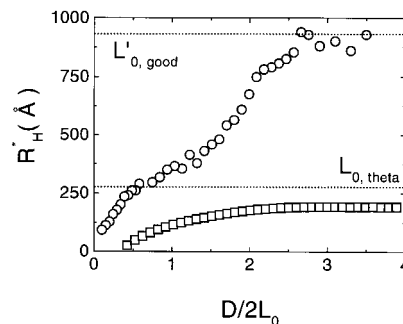


**Figure 8.** Equivalent hydrodynamic thickness,  $R_H^*$ , plotted against surface separation normalized by the unperturbed thickness of two polymer layers,  $D/2L_o$ , for PS–PVP polymer in a theta solvent (trans-decalin) and PB–PVP brush in a good solvent (tetradecane). Circles: PB–PVP in tetradecane. Squares: PS–PVP in trans-decalin. The  $R_H^*$  and  $L_o'$  for the PB–PVP system were normalized for differences of molecular weight and grafting density as described by eqs. (8) and (9). To identify normalization, these quantities are denoted  $R_{H'}^*$  and  $L_o'$ , respectively. Horizontal lines show the  $L_o$  and  $L_o'$  measured from the static force-distance profiles.

Figure 8 displays so little difference according to solvent quality.

There remain several challenges for future work. Clearly  $R_H^*$  is not a number to be taken literally as a thickness below which solvent ceases to flow; it would be desirable to have theoretical understanding of the actual profile of solvent flow. Secondly, quantitative understanding of how far the solvent velocity field penetrated within the polymer layers, especially under circumstances where  $D > 2L_o$  so that a layer of pure solvent should have separated the opposed polymers, is not yet in hand. Finally, it will also be interesting, in future work, to understand quantitatively why the hydrodynamic radius decreased so monotonically with surface separation, with no clear change of trend at the point,  $D = 2L_o$ , where the polymer layers began to overlap.

We dedicate this article to John D. Ferry on the occasion of his 85th birthday. We are indebted to Lenore L. Cai for measuring the static force-distance profile and to Jack F. Douglas and Svetlana A. Sukhishvili for invaluable discussions. This work was supported by grants from the Exxon Research and Engineering Corporation, the Ford Motor Co., and the National Science Foundation (Tribology Program).

## REFERENCES AND NOTES

1. J. D. Ferry, *Viscoelastic Properties of Polymers*, 3rd ed., Wiley, New York, 1980.

2. W. B. Russell, D. A. Saville, and W. R. Schowalter, *Colloidal Dispersions*, Cambridge University Press, New York, 1989.
3. J. Klein, E. Kumacheva, D. Mahalu, D. Perahia, L. J. Fetters, *Nature*, **370**, 634 (1994).
4. H. W. Hu and S. Granick, *Science* **258**, 1339 (1992); S. Granick and H. W. Hu, *Langmuir*, **10**, 3857 (1994).
5. L. Cai, J. Peanasky, and S. Granick, *Trends Polym. Sci.*, **4**, 47 (1996).
6. S. Alexander, *J. Physiol. (Paris)*, **38**, 977 (1997).
7. S. T. Milner, *Science*, **251**, 905 (1991).
8. S. Patel and M. Tirrell, *Annu. Rev. Phys. Chem.*, **40**, 597 (1989).
9. J. Klein, *J. Chem. Soc. Faraday Trans. I*, **79**, 99 (1993); J. Klein, Y. Kamiyama, H. Yoshizawa, J. N. Israelachvili, G. H. Fredrickson, P. Pincus, and L. J. Fetters, *Macromolecules*, **26**, 5552 (1993).
10. O. Reynolds, *Philos. Trans. R. Soc. Lond.*, **177**, 157 (1886).
11. J. N. Israelachvili, *Pure Appl. Chem.*, **60**, 1473 (1988).
12. J. M. Georges, S. Millot, J. L. Loubet, and A. Tonck, *J. Chem. Phys.*, **98**, 7345 (1993).
13. J. Klein, *Annu. Rev. Mater. Sci.*, **26**, 581 (1996).
14. A. Dhinojwala and S. Granick, *Macromolecules*, **30**, 1079 (1997).
15. J. Peachey, J. Van Alsten, and S. Granick, *Rev. Sci. Instrum.*, **62**, 463 (1991).
16. J. Bandrup and E. H. Immergut, *Polymer Handbook*, 3rd ed., Wiley InterScience, New York, 1989.
17. L. Cai, *Nanorheology of Polymer Brushes*, Ph.D. Thesis, University of Illinois at Urbana-Champaign (1997).
18. A. Dhinojwala, L. Cai, and S. Granick, *Langmuir*, **12**, 4537 (1996).
19. D. Y. C. Chan and R. G. Horn, *J. Chem. Phys.*, **83**, 5311 (1985).
20. J. N. Israelachvili, *J. Colloid Interface Sci.*, **110**, 263 (1986); J. N. Israelachvili, *Colloid Polym. Sci.*, **264**, 1060 (1986).
21. G. H. Fredrickson and P. Pincus, *Langmuir*, **7**, 786 (1991).
22. A. Dhinojwala and S. Granick, *J. Chem. Soc. Faraday Trans.*, **92**, 619 (1996).
23. J. N. Israelachvili and S. J. Kott, *J. Colloid Interface Sci.*, **129**, 461 (1989).
24. J. P. Montfort and G. Hadziioannou, *J. Chem. Phys.*, **88**, 7187 (1988).
25. Y. Guéguen and V. Palciauskas, *Introduction to the Physics of Rocks* Princeton University Press, Princeton, NJ, 1994.
26. D. Van Meerwall, *Adv. Polym. Sci.*, **54**, 1 (1983).